FUNDAMENTAL FREQUENCY LIMITATIONS IN CURRENT-MODE SALLEN-KEY FILTERS

Hanspeter Schmid and George S. Moschytz

Signal and Information Processing Laboratory, Swiss Federal Institute of Technology,
Sternwartstrasse 7, 8092 Zürich, Switzerland. E-mail: hanspeter.schmid@isi.ee.ethz.ch

ABSTRACT

Single-amplifier filter biquads and especially Sallen-Key filters are widely used to build higher-order filter cascades. This paper investigates high-frequency current amplifier non-idealities and their effects on all-pole Sallen-Key filter biquads. It is shown that a non-ideal current amplifier input causes parasitic zeros in the filter transfer function, and thus imposes fundamental limitations on the realisable pole frequency. Design equations are given, providing compensation for the amplifier's port impedances and its phase lag, by predistortion of the component values. It is also shown how design specifications for a current-amplifier can be derived from the filter specification, minimising the amplifier's power dissipation. Finally, a video-frequency lowpass filter is discussed.

1. INTRODUCTION

Single-amplifier filter biquads are widely used for building discrete-component filters (e.g. in [1] and [2, Sec. XV]). Among these filters, the positive-feedback filters (normally called Sallen-Key filters) stand out, because they can realise all biquadratic filter functions, and because changes in the amplifier gain have no influence on the pole frequency [3]. It has recently been shown how these filters can be implemented in CMOS using current amplifiers and MOSFET resistors [4].

The amplifier used in Sallen-Key filters normally has a low gain (in the order of unity). Principally, it can be implemented in two ways: either by applying feedback to a high gain amplifier, or by using a low gain open-loop amplifier. While the former is easier to realise in voltage-mode (e.g. as an operational amplifier with negative feedback), the latter is easier to implement in current-mode (e.g. as a current-mirror based gain stage, or a current conveyor). The former method is more precise, while the latter provides greater bandwidth.

It is well known that feedback not only reduces (and stabilises) the gain of an amplifier, but also makes the input and output impedances of the amplifier more ideal [2, 5, 6]. Open-loop amplifiers are less ideal from this point of view. Normally their high-impedance terminals (voltage inputs or current outputs) are capacitive in the frequency range of interest, while the low-impedance terminals (current inputs or voltage outputs) are resistive, or even inductive. Furthermore, an open-loop amplifier may have a considerable phase lag in the frequency range of interest, which is not caused by one *dominant pole*, but by a *pole-zero cluster* at high frequencies, which cannot be accurately modelled enough by a one- or two-pole model.

It is common practice to overcome the effects of such non-idealities either by trial-and-error methods, or by adding further components to the circuit (as e.g. in [7]). In this paper we show how, for current-mode Sallen-Key filters, an analytical approach makes it possible to derive a simple, but very effective design procedure. The main features of the analysis are that it includes phase lag effects as well as non-ideal port impedances, and that it shows to what extent the non-ideality of the amplifier's port impedances limits the maximum realisable pole frequency.

2. CURRENT-MODE SALLEN-KEY FILTERS

Fig. 1 shows a general current-mode Sallen-Key filter structure which can be used to implement a lowpass (LP), two different bandpass (BP1, BP2) and a highpass (HP) second-order transfer function.

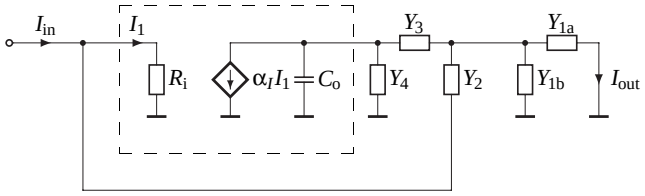

Figure 1: Sallen-Key filter structure (LP, BP and HP)

The Sallen-Key filter in Fig. 1 is built around a low-gain current amplifier with finite input admittance (R_{i}, resistive) and low, but not zero output admittance (C_{o}, capacitive). Although a current amplifier has been chosen in this paper, the same analysis is also valid for a voltage amplifer with input capacitance C_{o} and output resistance R_{i} [8]. Note that the gain α_I of the current amplifier must be negative in order to produce positive feedback, since a voltage-controlled voltage source (VCVS) is dual to a current-controlled current source (CCCS) having the opposite sign. (The reason for this is the conventional definition of the CCCS's output current direction.)

	$Y_{1\text{a}}$	$Y_{1\text{b}}$	Y_2	Y_3	Y_4	R_{i}	C_{o}
LP	R/n	0	C/m	Rn	Cm	R/ρ	C/κ
BP1	C/m	R/n	C/m	Rn	Cm	R/ρ	C/κ
BP2	R/n	C/m	R/n	Cm	Rn	R/ρ	C/κ
HP	C/m	0	R/n	Cm	Rn	R/ρ	C/κ

Table 1: Filter components

Table 1 shows how the admittances in Fig. 1 have to be chosen in order to realise the three different filter functions. The resistors and capacitors are expressed in terms of geometrical means (R, C) and component spread factors (m, n), because this leads to independent expressions for the *ideal* pole frequency ω_{pi} and the

ideal pole quality factor $q_{\mathrm{p\,i}}$. The amplifier's non-ideal port admittances are expressed in terms of R, C and of the impedance level factors $\rho = R/R_{\mathrm{i}}$ and $\kappa = C/C_{\mathrm{o}}$, which would be infinite for an ideal amplifier.

Open-loop current amplifiers normally do not have one dominant pole, but a cluster of poles and zeros at high frequencies. Thus there is no general model for the amplifier's phase lag valid over the whole frequency range of interest. Nevertheless, if the phase lag of the amplifier at the filter's pole frequency is reasonably small (say around ten degrees), its effects on the pole location can be approximated by using a linear phase lag (constant group delay) model. Then

$$\alpha_I(s) = \alpha_{I\,(\mathrm{s}=0)} \cdot e^{(-\phi RCs)} \,. \tag{1}$$

Here s is the complex frequency normally written as $s = \sigma + j\omega$, and ϕ is the phase lag at $\omega = 1/(RC)$, which is the pole frequency of the LP and HP filters, and close to the pole frequencies of the two BP filters (see equations (2_{LP})–(2_{HP})). The resulting non-linear filter transfer function can be linearised by setting $\phi = 0$ in the numerator (this must be done, because the phase lag model is only accurate in the region of the pole frequency, but not around the frequencies of the zeros) and by expanding the denominator as a Taylor series in s, cancelling all terms of order 3 and higher. This approximated filter transfer function allows a prediction of the shift of ω_{p} and q_{p} for all amplifier non-idealities, as given in the next section.

3. POLE SHIFTS

Ideally, the pole of the LP filter lies at

$$(\omega_{\mathrm{p\,i}}, \frac{1}{q_{\mathrm{p\,i}}}) = \left(\frac{1}{RC},\ \frac{m^2n^2 + m^2 + (\alpha_I + 1)}{mn}\right) . \tag{2_{LP}}$$

(The equations for the bandpass and highpass filters can be found in the Appendix.) The pole quality factor of (2_{LP}) can be written as

$$\frac{1}{q_{\mathrm{p\,i}}} = \frac{1}{mn} + mn + \frac{1}{n}\left(\frac{\alpha_I}{m} + m\right) .$$

It can easily be seen that $1/mn + mn \geq 2$, with equality for $mn = 1$. $q_{\mathrm{p\,i}}$ can be made larger than $1/2$ only if $1/n \cdot (\alpha_I/m + m)$ is negative, which is the case for $m \leq \sqrt{-\alpha_I}$,[1] and since $|\alpha_I|$ should not become too high, n should also be limited. In practice, m and n should be chosen such that $mn \approx 1$, $m \lesssim 1$, and n is reasonably small (on the order of unity).

Similar rules for choosing m and n can be derived for the other filters. From (2_{BP1}): $mn \approx \sqrt{2}$ and $m \lesssim 1$ for a reasonably small n. From (2_{BP2}): $mn \approx 1/\sqrt{2}$ and $n \gtrsim 1$ at a reasonably large m (on the order of unity). From (2_{HP}): $mn \approx 1$ and $n \gtrsim 1$ at a reasonably large m.

The three non-idealities (finite R_{i}, non-zero C_{o} and non-zero ϕ) shift the poles towards lower frequencies, where

$$\frac{\omega_{\mathrm{p}}^2}{\omega_{\mathrm{p\,i}}^2} = \frac{\rho\kappa mn}{\rho\kappa(mn - \phi\alpha_I) + \rho n + (\kappa m + 1)(n^2 + 1)} . \tag{3_{LP}}$$

[1] Remember that $\alpha_I < 0$.

The pole quality factors can also be expressed in terms of ρ, κ and ϕ, but here it is less obvious what happens to q_{p}:

$$\frac{1}{q_{\mathrm{p}}} = \frac{\rho\kappa(m^2n^2 + m^2 + (\alpha_I + 1)) + \rho m(n^2 + 1) + \kappa n}{\sqrt{\rho\kappa mn}\sqrt{\rho\kappa(mn - \phi\alpha_I) + \rho n + (\kappa m + 1)(n^2 + 1)}} . \tag{4_{LP}}$$

However, if $\phi = 0$ and either ρ or κ is assumed infinite, all expressions (4_{LP})–(4_{HP}) can be brought into the form

$$\frac{1}{q_{\mathrm{p}}} = \frac{1}{q_{\mathrm{p\,i}}} \cdot k_1 + k_2$$

where $k_1 < 1$ and $k_2 > 0$. It can be seen that $k_1 \approx 1$ for small component spreads, therefore non-ideal amplifier port impedances normally *decrease* the pole quality factor q_{p}. On the other hand, an amplifier phase lag *increases* the pole quality factor. This behaviour has also been observed in g_m-C filters [7].

4. PARASITIC ZEROS

There is a non-ideal effect which affects filter performance more than the (predictable) pole shifts, namely the parasitic zero or zeros caused by a finite ρ.

$$(\omega_{\mathrm{z}}^2, q_{\mathrm{z}}) = \left(\frac{1}{R^2C^2},\ \frac{-\rho\alpha_I m}{n\left(m + \frac{1}{\kappa}\right)},\ \sqrt{-\rho\left(m + \frac{1}{\kappa}\right)\alpha_I mn}\right) , \tag{$5_{\mathrm{LP,\,BP1}}$}$$

$$\omega_{\mathrm{z}} = \frac{1}{RC}\,\frac{1}{mn + \frac{n}{\kappa} - \rho\alpha_I m} . \tag{$5_{\mathrm{HP,\,BP2}}$}$$

The effects on the filter transfer function differ:

4.1. Lowpass filter (LP)

The complex pair of zeros causes the transfer function (TF) to become constant for frequencies above ω_{z}, and the minimum stopband attenuation A_{stop}, with respect to the passband attenuation A_{pass}, becomes $A_{\mathrm{stop}}/A_{\mathrm{pass}} \approx -\rho\alpha_I/n$ (for $\kappa \gg 1/m$). Since α_I is normally on the order of unity, the ratio $\rho/n = R_{1\mathrm{a}}/R_{\mathrm{i}}$ must be larger than the (given) ratio $A_{\mathrm{stop}}/A_{\mathrm{pass}}$.

For a certain frequency, the product RC is constant. Making $R_{1\mathrm{a}} = R/n$ larger (for the same n) therefore means making C smaller. However, C cannot be made arbitrarily small, both because this increases the filter's sensitivity to variations of C_{o}, and because of matching considerations. A good rule of thumb is to choose $\kappa \approx 10 \cdot \max(m, 1/m)$.

The resistance of the low-impedance terminal therefore imposes fundamental limitations on the filter's pole frequency, and the highest achievable frequency for a certain stopband attenuation is

$$\omega_{\mathrm{p\,max}} \approx \frac{A_{\mathrm{pass}}}{10 \cdot \max(m, 1/m) C_{\mathrm{o}} \cdot \max(n, 1/n) R_{\mathrm{i}} \cdot A_{\mathrm{stop}}} , \tag{6}$$

which reaches a maximum at $m = n = 1$. Note that it is not necessary to add a further safety margin, since the current amplifier normally has an attenuation of its own at frequencies above the zero frequency.

4.2. Bandpass filter (BP1)

Here the complex pair of zeros causes the TF to *rise 20 dB per decade* at frequencies above ω_z, until it flattens out again, at a gain of 1, because of a third high-frequency pole, which was previously cancelled from the Taylor series. Since ω_z/ω_p is in the order of $\sqrt{\rho}$, the filter's gain reaches unity at a frequency of about $\rho\omega_p$. *This may well make the filter useless for practical applications.*

4.3. Bandpass filter (BP2)

The single zero makes the TF constant for frequencies below ω_z, at a magnitude of approximately $\sqrt{2}\,\rho m$. Here it is a matter of convenience and interpretation to which level this should be referred, but the same fundamental frequency limitations occur as in the LP case.

4.4. Highpass filter (HP1)

In this case, the single zero changes the slope of the TF from 40 dB per decade to 20 dB per decade for frequencies below ω_z. Again, the minimum capacitance to be used in the feedback network and the filter specifications impose frequency limitations, although in this case the dependance of the maximum frequency on the specifications is more complicated.

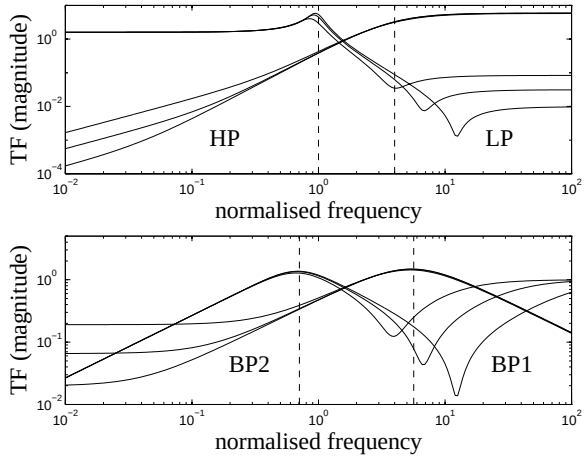

Figure 2: Transfer functions (TF) of the LP, BP1, BP2 and HP filters. The dashed lines indicate the different ω_{pi}.

To clarify, Fig. 2 shows the transfer functions of all four filters, where $m = 0.6$, $n = 1$, $\alpha_I = -1.6$, $\kappa = 30$ and $\rho = 10, 30, 100$. The magnitudes of HP and BP2 have been multiplied by 4, and different pole frequencies have been chosen, both for graphical reasons only. The effects of the parasitic zeros can be seen clearly in all four cases. It is also visible that the LP filter has by far the highest q_{pi}, which already follows from (2_{LP})–(2_{HP}).

5. PRACTICAL EXAMPLE

As an example, consider a Sallen-Key lowpass filter biquad with $f_p = 16.58\,\text{MHz}$, $q_p = 4$, and a stopband attenuation of at least 30 dB.[2]

A single-ended CMOS class AB second-generation current conveyor (CCII) is used as current amplifier. It is similar to the balanced CCII presented in [4], and is based on a concept presented by Erik Bruun in [9, Chap. 11.5, Fig. 3(d)]). Simulations using reliable high-frequency transistor models[3] show that the current input of the CCII has a resistance on the order of 100 Ω, depending on the bias current, while the current output has a capacitance of $C_o \approx 0.05\,\text{pF}$.

The choice of "optimum" values of m, n and α_I really depends on which sensitivity criterium should be optimised. A detailed explanation of such an optimisation is out of the scope of this paper, thus we choose sensible values according to the criteria given in Section 3 without further explanation: neglecting the passband attenuation ($A_{pass} \approx 0\,\text{dB}$), and assuming $\max(m, 1/m) \approx 2$ and $\max(n, 1/n) \approx 1.25$, it follows that the input resistance of the CCII must be $R_i = 240\,\Omega$. Then $C = \max(m, 1/m)C_o = 1\,\text{pF}$, and $R = 9.6\,\text{k}\Omega$ from (2_{LP}). The CCII used for the simulations has a gain of $\alpha_I = -1.57$. If $n = 1$ is chosen, as suggested in the previous section, it follows that $m = 0.6$. However, if the filter is built using these values, the actual pole frequency and pole quality factor will deviate from the ideal. Since the CCII has a phase lag of 7 degrees at 16.58 MHz, the equations (3_{LP}) and (4_{LP}) predict $f_p = 13.6\,\text{MHz}$ and $q_p = 3.1$. This corresponds well to the simulated $f_p = 13.6\,\text{MHz}$ and $q_p = 3.0$.

The pole frequency can be corrected by making R smaller, either in two or three iterative steps, or by replacing ρ by R/R_i in (3_{LP}) and solving for R. This results in $R = 7.85\,\text{k}\Omega$ (and therefore $\rho = 32.7$). Due to other non-ideal effects, the pole frequency $f_p = 16.2\,\text{MHz}$ is still slightly low, but close enough such that a new value for $1/R$ can be linearly extrapolated,[4] resulting in $R = 7.58\,\text{k}\Omega$ and a filter having the correct f_p.

The problem of the low q_p remains. A similar procedure can now be applied to (3_{LP}), solving for a new value of $n = 0.9$. Now the simulated filter has a $q_p = 3.9$, but f_p has not been changed, since the two are orthogonal to each other. Linear extrapolation suggests using $n = 0.89$, which gives the correct q_p.

	simulated	corrected	ideal
f_p [MHz]	13.6 (−18%)	16.2 (−2%)	16.58
q_p	3.0 (−25 %)	3.9 (−2.5 %)	4.0

Table 2: Simulated ω_p and q_p of the LP transfer function

Discussion and Design Procedure: Table 2 shows the ideal values of f_p and q_p and the simulated values with ideal components ("simulated") and with components calculated using equations (3_{LP}) and (4_{LP}) ("corrected"). The values after linear interpolation are not shown, since they differ from the ideal values by less than 0.2%. The stopband attenuation of the filter reaches its maximum of 35 dB at about 400 MHz, which is better than expected. The reason for this is that the gain of the CCII has already decreased by 7 dB at this frequency.

This example shows that the equations (3_{LP}) and (4_{LP}) themselves provide a very good means of designing a filter, even if only R_i, C_o and the phase lag at f_p of the amplifier are known, and no accurate simulations of the whole filter can be made. Non-idealities of the CCII other than input resistance, output capacitance and phase lag, e.g. attenuation at high frequencies or parasitic poles and zeros in the impedances, can also be accounted for if

[2] Although it is rather small, this attenuation already results in 60 dB stopband attenuation for a cascade of two biquads in a 4th-order filter.

[3] BSIM 3v2 model of a 0.6μm process

[4] Note that f_p is a linear function of $1/R$, not R.

the whole filter can be simulated and one additional interpolation step is made.
The design procedure can now be summarised as follows:

1. Calculate m, n and α_I from (2_{LP}), taking into account the discussion in the beginning of Section 3 and possibly sensitivity considerations. Note that $1/m$ and n need to be large for low sensitivity [3], thus there is a sensitivity–speed tradeoff.
2. Calculate R, C and the product $R_{\mathrm{i}}C_{\mathrm{o}}$ from (6) and design the CCII accordingly, such that its phase lag at f_{p} is not greater than about ten degrees. Note that since low input resistance and low phase lag at high frequencies must be paid for by higher power consumption, designing the CCII's R_{i} and ϕ close to the limits actually means minimizing its power dissipation.
3. Correct f_{p} by changing R according to (3_{LP}).
4. If possible, simulate the filter both with ideal components values and with predistorted values, and extrapolate $1/R$ as a function of f_{p}.
5. Correct q_{p} by changing n (or m) according to (4_{LP}).
6. Simulate, and extrapolate n (or m) as a function of q_{p}.

Similar design procedures can easily be derived for the BP2 and HP filter.

6. CONCLUSION

We have analytically shown how current (and voltage) amplifier non-idealites affect the transfer functions of the four basic allpole Sallen-Key filter biquads: Non-ideal port impedances decrease the pole frequency ω_{p} and the pole quality factor q_{p}, while an amplifier phase lag decreases ω_{p} but increases q_{p}.

Still more importantly, a non-ideal amplifier input causes parasitic zeros in the transfer functions, which imposes *fundamental limitations on the maximum realizable pole frequency*, and even makes one of the two bandpass filter structures almost useless for the building of integrated high-frequency filters.

Design equations for all four filters are presented, and a low-pass filter example using a CMOS current conveyor (CCII) is designed. A simple design procedure for the predistortion of the filter components is given, and it is shown how upper bounds on the current amplifier non-idealities can be derived from the filter specifications, and how these bounds can be used to optimise the CCII with respect to power consumption.

7. ACKNOWLEDGEMENTS

We would like to thank D. Lím and M. Helfenstein for their valuable comments on our work, and our students R. Schwendener and O. Lamparter, who encountered the parasitic zeros in their semester project [10], for the many stimulating discussions.

8. APPENDIX

$$(\omega_{\mathrm{p\,i}}, \frac{1}{q_{\mathrm{p\,i}}}) = \left(\frac{1}{\sqrt{2}\,RC}, \frac{m^2n^2+m^2+(\alpha_I+2)}{\sqrt{2}mn}\right), \qquad (2_{\mathrm{BP1}})$$

$$\left(\frac{\sqrt{2}}{RC}, \frac{m^2n^2(\alpha_I+2)+m^2+1}{\sqrt{2}mn}\right), \qquad (2_{\mathrm{BP2}})$$

$$(\omega_{\mathrm{p\,i}}, \frac{1}{q_{\mathrm{p\,i}}}) = \left(\frac{1}{RC}, \frac{m^2n^2(\alpha_I+1)+m^2+1}{mn}\right). \qquad (2_{\mathrm{HP}})$$

$$\frac{\omega_{\mathrm{p}}^2}{\omega_{\mathrm{p\,i}}^2} = \frac{\rho\kappa mn}{\rho\kappa(mn-\frac{1}{2}\phi\alpha_I)+\rho n+\frac{1}{2}(\kappa m+1)(n^2+1)+\frac{\kappa}{2m}}, \qquad (3_{\mathrm{BP1}})$$

$$\frac{\rho\kappa mn+\frac{\kappa mn^2}{2}}{\rho\kappa(mn-\phi m^2n^2\alpha_I)+(\rho n+n^2)(m^2+1)+\kappa mn^2}, \qquad (3_{\mathrm{BP2}})$$

$$\frac{\rho\kappa mn}{\rho\kappa(mn-\phi m^2n^2\alpha_I)+(\rho n+n^2)(m^2+1)+\kappa mn^2}, \qquad (3_{\mathrm{HP}})$$

$$\frac{1}{q_{\mathrm{p}}} = \frac{\rho\kappa(m^2n^2+m^2+(\alpha_I+2))+\rho m(n^2+1)+\kappa n}{\sqrt{\rho\kappa mn}\sqrt{\rho\kappa(2mn-\phi\alpha_I)+2\rho n+\kappa m(n^2+1)+\frac{\kappa}{m}+(n^2+1)}}, \qquad (4_{\mathrm{BP1}})$$

$$\frac{\rho\kappa(m^2n^2(\alpha_I+2)+m^2+1)+2\rho mn^2+\kappa n(m^2n^2+m^2+1)+mn^3}{\sqrt{(2\rho+n)\kappa mn}\sqrt{\rho\kappa(mn-\phi\alpha_I m^2n^2)+\rho n(m^2+1)+n^2(m^2+\kappa m+1)}}, \qquad (4_{\mathrm{BP2}})$$

$$\frac{\rho\kappa(m^2n^2(\alpha_I+1)+m^2+1)+\rho mn^2+\kappa n(m^2+1)}{\sqrt{\rho\kappa mn}\sqrt{\rho\kappa(mn-\phi\alpha_I m^2n^2)+\rho n(m^2+1)+\kappa mn^2+n^2(m^2+1)}}. \qquad (4_{\mathrm{HP}})$$

9. REFERENCES

[1] R. P. Sallen and E. L. Key, "A practical method of designing RC active filters," *IRE Trans. CT*, vol. CT-2, no. 1, pp. 74–85, Mar. 1955.

[2] Wai-Kai Chen, *The Circuits and Filters Handbook*, CRC Press, Inc., 1995.

[3] G. S. Moschytz, "Single-amplifier active filters: A review," *Scientia Electrica*, vol. 26, no. 1, pp. 1–46, 1980.

[4] Hanspeter Schmid and George S. Moschytz, "Tunable CCII-MOSFET-C filter biquads for video frequencies," in *Proc. ECCTD*, Budapest, 1997, vol. 1, pp. 82–87.

[5] Arie Arbel, "Negative feedback revisited," *Analog Int. Circ. and Signal Proc.*, vol. 10, no. 3, pp. 157–178, Aug. 1996.

[6] Paul R. Gray and Robert G. Meyer, *Analysis and Design of Analog Integrated Circuits*, John Wiley & Sons, New York, 3 edition, 1993.

[7] Chung-Chih Hung, Kari A. I. Halonen, Mohammed Ismail, Veikko Porra, and Akira Hyogo, "A low-voltage, low-power CMOS fifth-order elliptic GM-C filter for baseband mobile, wireless communication," *IEEE Trans. CAS Video Techn.*, vol. 7, no. 4, pp. 584–593, Aug. 1997.

[8] G. S. Moschytz and A. Carlosena, "A classification of current-mode single-amplifier biquads based on a voltage-to-current transformation," *IEEE Trans. CAS–II*, vol. 41, no. 2, pp. 151–156, Feb. 1994.

[9] John Lidgey, Chris Toumazou, Alison Payne, Doug C. Wadsworth, Sittichai Pookaiyaudom, and Erik Bruun, "Tutorial 10: Current-mode analog signal processing; part 2: Current conveyors," in *Proc. ISCAS*, London, 1994, pp. 569–641.

[10] Rico Schwendener and Oliver Lamparter, "Integrated tunable high-frequency filters," *Semester Project*, Sig. Inf. Proc. Lab., ETH Zürich, 1997, (in German).